New York University

Ocean Models: Heat, Challenges, and Significance

Itxaso Ezcurra-Taiganedes, Reese Burns, Angela Chi, Amy Gao

MATH-UA 228: Earth's Atmosphere and Climate

Professor Olivier Pauluis

13 May 2025

Table of Contents

1. ***Introduction (Itxaso)***

Insofar as human knowledge goes, the Earth is unique in its ability to support life. The role that water, stored in this blue planet's vast oceans, plays in maintaining or fostering this life is key. Not only do our oceans store energy in the form of heat and nutrients, but they also support vast and complex biological and mechanical processes that are part of the balanced dance we know as Earth's climate.

In this paper, we explore how ocean dynamics, such as heat transport and circulation, contribute to climate regulation. To do so, let's discuss the basic and unique properties of water, or H_2O:

High Heat Capacity

Owing to its molecular structure, water has one of the highest heat capacities of the common substances found on Earth at $4.184\,J/g°C$ (Libretexts). This means that it takes a relatively significant amount of time and energy to warm one gram of water by one degree Celsius. In other words, water can take in relatively significant amounts of solar energy before changing temperature itself. In our ocean-climate systems, this absorptive quality of water shows up in various spatial and temporal scales. Firstly, the presence of water will moderate any extremes in temperature. Seeing that the Southern hemisphere is 80% ocean, whereas 60% of the Northern hemisphere is ocean, the seasonal temperature cycle which flows with the Earth's rotation and tilt with relation to the sun is much less pronounced in the South than the North (Vallis, 109). Secondly, the presence of water will induce a lad between maximum insolation and maximum temperatures. Thus, the Southern hemisphere not only sees less variation in temperature throughout the year, but also that maximum temperatures are seen later in the day and in the season (Vallis, 111).

The already high heat capacity of water is exacerbated in the context of the ocean because of the perturbation which occurs at the ocean's surface due to wind currents. The effective heat capacity of the oceans lies in what we know as the mixing layer - between 50 and 100 meters from the surface - which has a heat capacity which is 100 times higher than that of land. If this is not convincing enough, the heat capacity of the entire atmosphere corresponds to only 3 meters of the mixing layer's heat capacity (Vallis, 108-109).

Unique Phase Change Properties

While liquid water's phase change into gaseous form plays a critical role in atmospheric circulation - due to its high latent heat of vaporization - the forming of ice within Earth's ocean is just as important for driving oceanic circulation. This is because of the fact that ice is made up solely of water molecules, whereas ocean water contains dissolved salt particles. Thus, when sea ice forms, taking in only water molecules and leaving behind salt, the surrounding water becomes saltier and thus less dense. This phenomenon, where parcels of free molecules with higher density lay above less dense parcels, drives the process we know as convection. This plays a key role in the global Thermohaline Circulation which we will delve into later in this paper. Additionally, though often taken for granted, the fact that the solid state of water is less dense than the liquid phase not only enables this convective process but also provides insulation to the vast array of living organisms which call the oceans home.

Albedo

Lastly, the albedo - or solar reflectivity - of water depends highly on its phase state. While ice and snow have a relatively high albedo of 70-90%, ocean water has a very low albedo of 6-10% - even lower than that of land (Earth 103: Earth in the Future). This has important repercussions for the exchange of heat between solar radiation and the Earth's surface. More precisely, processes of ice formation and melting are sensitive to changes in temperature, establishing two interconnected positive feedback loops: (1) more ice brings more albedo which lowers surface temperatures that fuel more ice formation, and (2) less ice brings less albedo which raises surface temperatures that fuel more melting (Vallis, 122).

All of these properties contribute to the complex and interconnected nature of the oceans' role in climate. But because of its vast size, and still widely unknown mechanisms of circulation, the understanding of this role is still limited. Mathematicians, physicists, and other scientists have built simplified models of the ocean in order to better understand its basic functioning and effect on climate systems.

Modeling a Simple Ocean

The most basic simplification that allows for us to deduce certain interactions between the ocean and the climate is the assumption that the ocean is a singular and uniform entity (a blob). Viewing the oceans as a homogeneous body of salt water allows us to form a basic understanding of the heat buffer effect of ocean water on climate systems. We will thus build a basic mathematical model for the damping effects of a simple ocean:

By assuming that the cooling rate of the surface varies linearly with temperature - ie the hotter the object, the faster it releases heat - this model will take into account the following variables: S as our source of heat, T as the temperature, t for time, C for the heat capacity of the system, and λ, our constant determining the rate of cooling (Vallis, 113). We establish this ordinary differential equation which relates the temperature change associated to a body with relation to its inherent cooling tendencies and a heat source:

$$C * \frac{dT}{dt} = S - \lambda * T$$

The solution to this ODE is as follows:

$$T(t) = \frac{S}{\lambda} + T_o * e^{-\lambda t/C} = \frac{S}{\lambda} + T_o * e^{-t(\frac{\lambda}{C})}$$

This equation tells is that if there is a perturbation to the system (T_o), it will decay on the timescale $\frac{C}{\lambda}$. Since there exist estimates for the rate of cooling for a mixing layer of 100m, we can calculate this timescale: for $\lambda = 15\ W/m^2K$ this timescale is a little less than a year meaning it takes about a year for the mixing layer to both absorb and give out heat. This also means that for any timescales longer than a year, the ocean mixing layer will not contribute to the damping of the system because it will have already changed temperature itself. This simplistic analysis shows us that the oceans effectively act as a heat buffer for the global temperatures within periods shorter than a year by absorbing heat and releasing it at lagged timescales.

This being said, simplifying the vast complexities of our planet's oceans in such a way leads to wide uncertainties. Such a simplified view is not fully representative of the complex processes that take place like lateral variations and possible diurnal temperature variations. In reality, there are much more complex processes that allow for the ocean to drive the redistribution of heat at global levels. So though we can attain a simple understanding of ocean-climate interactions through vast simplifications, we look to more complex models for developing a better understanding of the role of the oceans on Earth's climate.

2. Zanna et al 2019: Introduction & Analysis (Reese)

To build on this understanding, we conducted an exploratory data analysis using real-world data from the article *"Global Reconstruction of Historical Ocean Heat Storage and Transport"* (Zanna et al. 2019*)*, focusing on how specific oceanic variables influence climate-related factors. While the article highlights both global and regional trends in ocean heat content and transport, so our analysis aims to replicate, interpret, and further explore these patterns. Specifically, we examine how Latent Heat Flux (LHTFL) at the ocean's surface changes over time in relation to Sea Surface Salinity (SSS) and Temperature (SST).

About the Data

The real-world data used for our modeling comes from datasets specifically referenced in the *Zanna et al.* (2019) article: two from the *Estimating the Circulation and Climate of the Ocean* (ECCO) project and one from the *National Centers for Environmental Information* (NCEI). The ECCO datasets provide Sea Surface Salinity (SSS) and Temperature (SST) values, while the NCEI dataset contains Latent Heat Flux (LHTFL) data. Each dataset includes columns for timestamp (year-month-day) ranging from 1955-2017, latitude, longitude, and the respective variable (e.g. salinity, temperature, or latent heat flux).

To prepare the data for exploratory data analysis, we performed several preprocessing steps. First, we standardized column names across all datasets for consistency. Next, we masked invalid values (i.e. -1.00000e+23), which typically represent land areas rather than oceanic measurements. Finally, we selected the years 1992, 1997, 2002, 2009, and 2015 to capture a range of variability in oceanic conditions. These years correspond to different phases of the El Niño-Southern Oscillation (ENSO): 1992 represents a neutral year, 2002 and 2009 represent moderate ENSO events, and 1997 and 2015 correspond to extreme ENSO events. ENSO events are recurring climate patterns that affect SST across the East-Central equatorial Pacific Ocean. El Niño events are associated with eastward-spreading SST warming, while La Niña events involve westward-spreading SST cooling.

Exploratory Data Analysis

After collecting and preprocessing the data, we conducted an exploratory data analysis to better understand the contents and trends within each dataset. As a first step, we generated time-series plots showing the global monthly trends by year for each of the datasets below *(Figures 1.1-1.3)*.

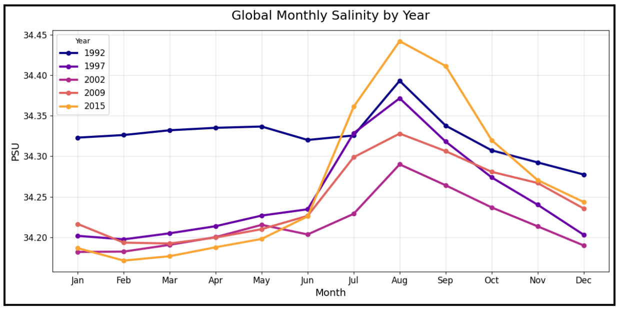

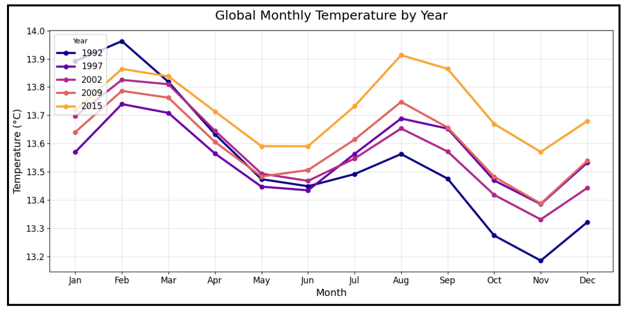

Figure 1.1

Figure 1.2

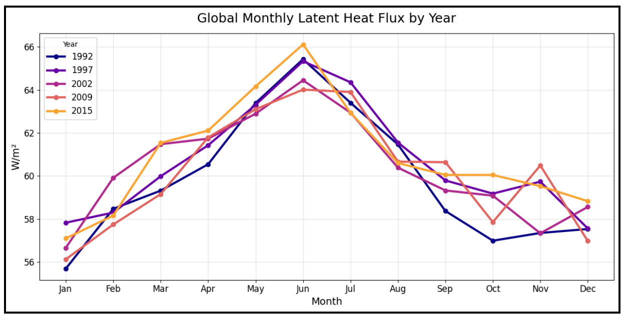

Figure 1.3

In *Figure 1.1*, we observe that salinity levels are generally highest during July through September and lowest from January through June. *Figure 1.2* shows that temperatures peak in February and decline steadily from September to December. And *Figure 1.3* illustrates how the most intense latent heat flux is from May to July, with a steady decrease through the remainder of the year, reaching the lowest transfer levels between October and January.

Second, we created global spatial plots with the Cartopy package to visualize geographic trends in each dataset. Initially, the raw spatial plots of sea surface salinity (SSS) and temperature (SST) did not reveal significant visual disparities across years. To better highlight changes, we computed anomaly maps by subtracting each ENSO event year's values (1997, 2002, 2009, and 2015) from the corresponding baseline values in 1992 at matching timestamps and coordinates.

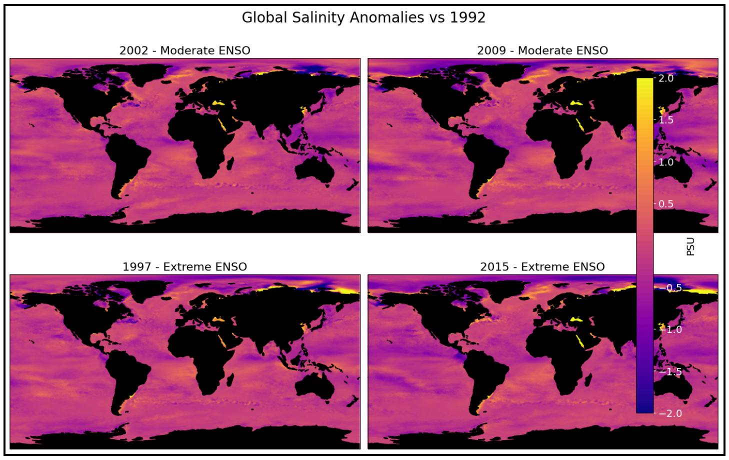

Figure 2.1

As shown in *Figure 2.1*, global salinity anomalies reveal several key patterns. Higher salinity levels (bright yellow) are observed in the subtropical oceans, likely due to increased evaporation. Lower salinity levels (dark purple) are concentrated in the equatorial Pacific, possibly due to enhanced rainfall and freshwater input during ENSO events. Additionally, strong salinity anomalies appear in coastal regions near large rivers (e.g. the Amazon and Ganges) and polar zones (e.g. Greenland and Antarctica), reflecting freshwater influx from river discharge and melting ice sheets.

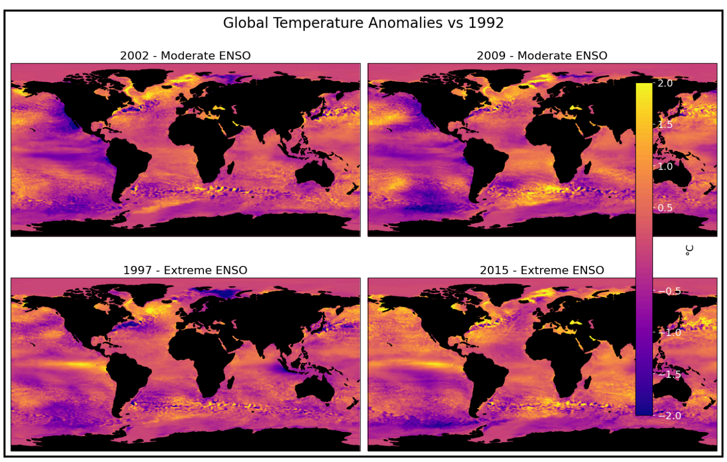

Figure 2.2

Figure 2.2 illustrates global temperature anomalies. Warmer temperatures (bright yellow) dominate much of the Pacific, Northern, and Indian Oceans. These warming patterns are likely driven by increased ENSO activity, long-term global warming, and possible weakening of the Atlantic Meridional Overturning Circulation (AMOC)–a topic explored later in this paper *(5. AMOC & Thermohaline)*. Cooler temperatures (dark purple) are visible in the North Atlantic, East Pacific, Southern Ocean, and along coastal margins, possibly due to upwelling or increased freshwater inputs in those regions.

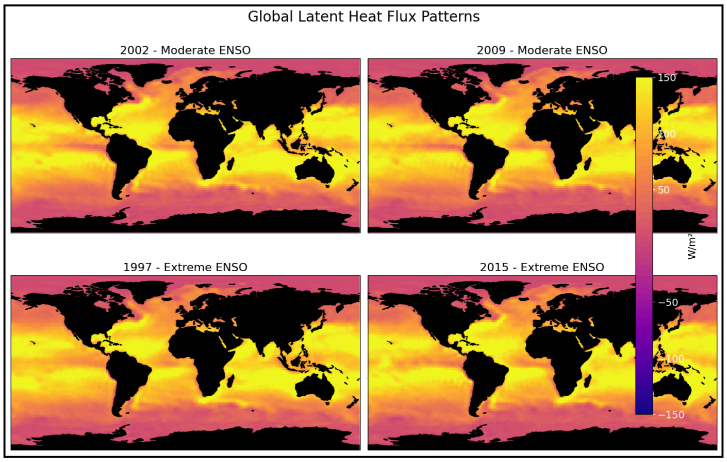

Figure 2.3

Finally, *Figure 2.3* shows global latent heat flux patterns. Higher latent heat flux (bright yellow) is seen in Subtropical Atlantic, West Pacific, and Indian Oceans, consistent with greater evaporation in these zones. Conversely, lower latent heat flux (dark purple) appears in the Polar, East Pacific, and coastal regions, likely caused by increased condensation and moisture convergence.

Since latent heat flux patterns are most prominent in subtropical regions, we further investigated the differences in heat transfer during El Niño years–specifically 2009 (moderate), 1997 (extreme), and 2015 (extreme).

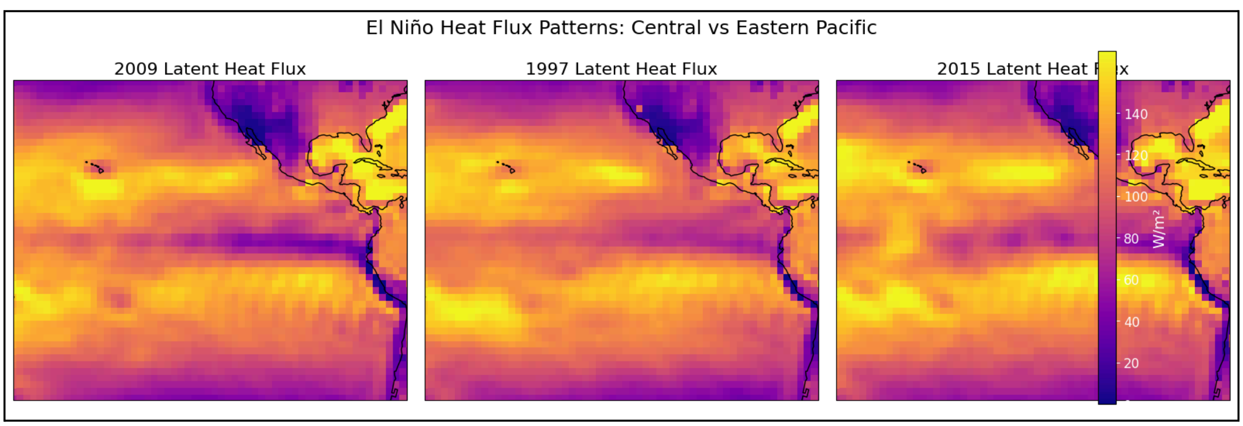

Figure 3

Figure 3 displays regional latent heat flux patterns across the Central and Eastern Pacific for each of these El Niño years. In 2009, the highest heat flux (bright yellow) is concentrated in the Central Pacific, suggesting a westward shift of warming and evaporation-driven energy transfer.

In contrast, both 1997 and 2015 exhibit broader and more intense latent heat flux in the Eastern Pacific, where increased surface warming and evaporation likely amplify the overall heat transfer in that region.

Our exploratory data analysis highlights key seasonal and spatial trends in salinity, temperature and latent heat flux of the ocean's surface across different ENSO years. We observed consistent seasonal cycles in all three variables globally, as well as notable spatial anomalies in the Pacific and polar regions. In particular, shifts in latent heat flux between the Central and Eastern Pacific during El Niño years reveal meaningful differences in how energy is redistributed across the ocean's surface. These patterns inform the next stage of our analysis, where we further quantify the relationships between these variables and compare trends across time and space.

Analysis & Comparisons

Building on the patterns observed in our exploratory analysis, we now examine the global change over time of latent heat flux (LHTFL) in the ocean's surface based on variables like sea surface salinity (SSS) and temperature (SST). First, we further prepared the data by merging all three datasets on timestamp, latitude, and longitude, and then grouping by month. As a disclaimer, the values computed in this analysis reflect the selection of years spanning neutral, moderate, and extreme ENSO events, combined with a global dataset that emphasizes tropical and southern ocean regions. Consequently, the patterns observed here reflect high climate variability and may not align with broader global ocean-atmosphere trends. With that in mind, we created a correlation heatmap to uncover the relationship between salinity, temperature, and latent heat flux *(Figure 4)*.

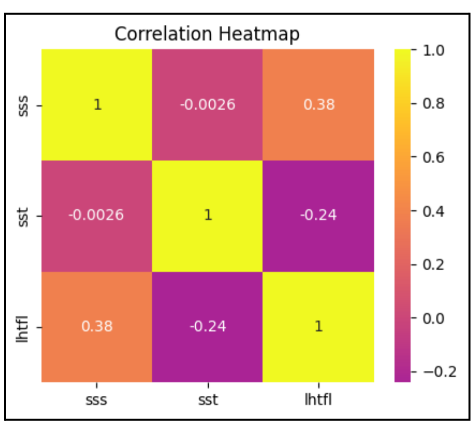

Figure 4

As shown in Figure 4, sea surface salinity (SSS) has moderate positive correlation ($r_{SSS} = 0.38$) with latent heat flux (LHTFL), suggesting that as salinity increases then heat flux also increases on average. This is likely due to higher salinity being associated with drier and warmer regions where evaporation rates and, thus, latent heat transfer are elevated. In contrast, sea surface temperature (SST) shows a moderate negative correlation ($r_{SST} =- 0.24$) with latent heat flux (LHTFL). This suggests that as surface temperatures rise then heat flux tends to decrease. This inverse relationship may be due to saturation effects: where warmer waters hold more moisture, reducing the evaporation and, thus, the amount of heat transfer.

Next, we visualized these correlation patterns using global density plots to examine how latent heat flux (LHTFL) clusters across different ranges of sea surface salinity (SSS) and temperature (SST) by month *(Figure 5)*.

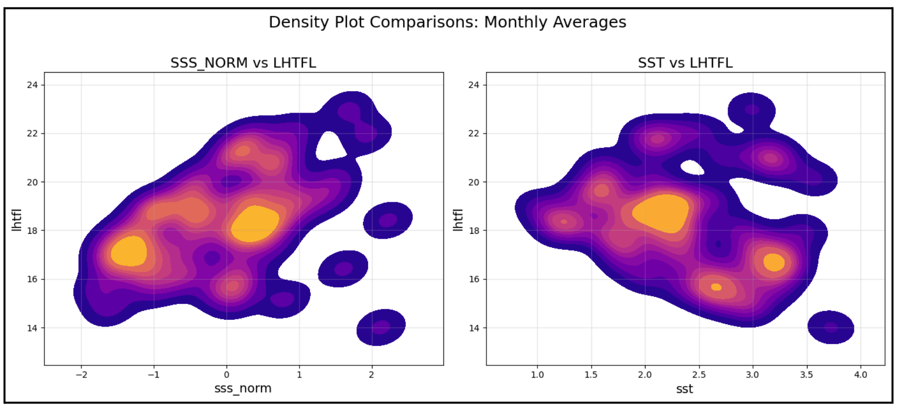

Figure 5

Figure 5 displays the global density of SSS and SST as a function of latent heat flux. In both plots, high-density regions (bright yellow) appear around average salinity and temperature values, suggesting that latent heat flux is generally concentrated under average ocean conditions. In the salinity plot (left), high salinity levels coincide with increased latent heat flux, likely reflecting persistent evaporation in drier regions. Conversely, low salinity values (dark purple) are associated with higher heat flux as well, possibly due to freshwater input and enhanced evaporation in those areas. In the temperature plot (right), warmer temperatures are associated with reduced latent heat flux. This may be due to ENSO-related decreases in wind and increases in humidity, which suppress evaporation. On the other hand, cooler temperatures also correspond with lower latent heat flux, potentially due to reduced evaporation capacity in colder waters.

These patterns reinforce the idea that latent heat flux is most stable under moderate conditions and sensitive to both extremes.

To further explore how these patterns vary across regions, we generated scatterplots of sea surface salinity (SSS) and temperature (SST) as a function of latent heat flux (LHTFL) during extreme El Niño years of 1997 and 2015 *(Figure 6)*.

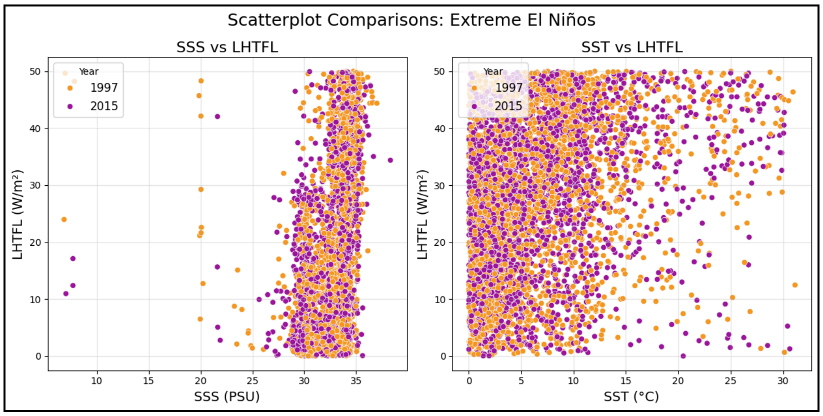

Figure 6

Figure 6 compares SSS and SST with latent heat flux specifically during these extreme ENSO years, with a focus on the Pacific, Atlantic, and Southern Oceans. In the salinity plot (left), there appears to be a weak, near-neutral correlation with latent heat flux–as data points show substantial overlap and no clear trend. This suggests that during extreme El Niño years, salinity may not fluctuate enough to significantly influence latent heat flux. In contrast, the temperature plot (right) reveals a broader spread and slight positive trend, particularly at higher temperatures. This indicates a weak positive correlation between SST and latent heat flux, where elevated temperatures may contribute to slightly increased heat transfer. These regional scatterplots highlight more localized and event-specific variability than what we observed in the global correlation heatmap, emphasizing that relationships between salinity, temperature, and latent heat flux can shift when focusing on anomaly years rather than long-term global averages.

Findings

Based on our analysis of what influences latent heat flux (LHTFL) at the ocean's surface, we found that sea surface salinity (SSS) shows no strong global correlation with latent heat flux. This suggests that salinity functions more as a passive tracer of long-term evaporation patterns than as a direct driver of latent heat exchange. However, regional analysis revealed that higher salinity levels are typically concentrated in subtropical regions with persistent evaporation (e.g. South Atlantic Ocean), while lower salinity levels in the equatorial Pacific are linked to freshwater influx and elevated flux rates, particularly during ENSO events. While salinity does not appear to significantly affect latent heat flux, it plays an important role in shaping ocean density when combined with temperature. These variations are key to driving Thermohaline Circulation, a topic explored later in this paper *(5. AMOC & Thermohaline)*.

In contrast, sea surface temperature (SST) demonstrates a moderate global positive correlation with latent heat flux. Warmer temperatures, especially in the tropical Pacific, correspond to increased latent heat transfer, though this relationship is somewhat nonlinear and influenced by wind and humidity conditions as well. During extreme ENSO years like 1997 and 2015, our plots show that elevated SST in the Eastern Pacific aligns with intensified latent heat flux, where cooler conditions in polar and upwelling zones coincide with reduced flux.

Overall, our modeling of data from Zanna et al. (2019) supports the conclusion that while salinity plays a secondary and regionally dependent role, latent heat flux is primarily influenced by temperature and regional climate dynamics. The strongest ocean-atmosphere coupling occurs in tropical regions (where warming drives evaporation) and southern high-latitude oceans (where cold conditions modulate flux through suppressed evaporation and increased freshwater input). These findings set the stage for understanding how sea surface anomalies, particularly in temperature, propagate into the ocean interior. This is a process Zanna et al. (2019) models through partial differential equations to estimate changes in ocean heat content (OHC).

3. ***Zanna et al 2019: Methodology (Angela)***

Zanna et al. 2019 investigate heat transport within ocean basins by comparing the predictions of a Green's Function (henceforth, GF) reconstruction of OHC, i.e. their model, with direct estimates of OHC change from observational datasets of interior temperatures. The comparison of OHC reconstruction with direct estimates enables researchers to *infer* the role of changes in ocean transport in shaping patterns of OHC over time. This methodological step is necessary due to the various intrinsic difficulties of gathering data about the ocean. To this end, they focus on the Atlantic Ocean as a particularly good candidate of study because previous observations of this region are densest, and the contrast in storage between high and low latitudes is large. In this section, we describe their methodology and justification for their methods, which also serves as the foundation for our own findings as outlined in the previous section.

On the framework we adopted, high latitudes are difficult to measure and model due to deep water formation and large decadal variability signals in SSTs. Thus, Zanna et al. specify that the methods they use cannot fully capture the changes in ocean processes in these areas, although some partial conclusions were drawn above, described in the previous section. With this acknowledgement of inherent limitations, we now turn to a description of their methodology.

PDEs for OHC

In their study, passive heat uptake is measured under a time-mean GF assumption. These GFs are calculated over zonally averaged 10 degree latitudinal bands at 22 vertical levels. Their GF reconstruction combines time-dependent SSTs with a time-independent representation of ocean-transport processes, which represents ocean pathways in terms of distribution of timescales and probability. The two central equations – PDEs, as previously stated, unlike ODEs used for simple ocean models – are provided below (Zanna et al. 2019):

$$OHC(V_R, t) = \int_{V_R} d\mathbf{r}\, c_p\, \rho(\mathbf{r}, t) \int_{1871}^{t} dt' \int_{S} d\mathbf{r}'\, G(\mathbf{r}, t - t'; \mathbf{r}')\, T^S(\mathbf{r}', t'), \qquad \textbf{[1]}$$

$$OHU(r_i', V_R, t) = \int_{V_R} d\mathbf{r} \int_{1871}^{t} dt'\, c_p\, \rho(\mathbf{r}, t)\, G(\mathbf{r}, t - t'; r_i')\, T^S(r_i', t'), \qquad \textbf{[2]}$$

The first PDE estimates *ocean heat content* overall while the second PDE focuses specifically on *ocean heat uptake*. In both, the operator G(r, t–t' ; r') is the Green's function used to estimate change in heat across the surface, and T^S(r', t') represents SST anomalies per patch (r) and time (t), i.e. the change in sea surface temperature at a particular place and time. We discuss each PDE in detail below.

Equation [1] is a convolution for OHC estimates in the interior over V_R, where V_R is the total volume over all patches (*r*) in their model from 1871 to a particular time (*t*). 26 surface patches are used to connect the surface to the interior, defined based on density in each basin, thus r_i ranges from 1 to 26, and *R* represents all of the patches. In [1], c_p = 3,992 J/(kgC), the specific heat capacity of the ocean; *S* represents the surface of the ocean; *r*', *r* represent the location of a particular patch; *t'*, *t* represent a particular time.

The surface integral in [1] is discretized over 26 surface regions, each denoted by r_i with $i = 1, 2, 3, \ldots, 26$. These are the patches previously described. The convolution in [1] assumes that SST anomalies before 1871 must be zero; therefore, the ocean circulation must be equilibrium. This set-up is necessary due to human limitations and computational cost, but we'll talk more about how to model ocean circulation in the next section (*4. Stewart & Hogg*), i.e. by "spinning up". This is not central to Zanna et al. (2019), however, so we won't go further into detail here.

What *is* relevant for our purposes and findings, however, is the method of calculating density, i.e. $\rho(r, t)$ in kg/m^3, which occurs in the outermost integral (V_R). This value is calculated by Zanna et al. at (r, t) using Temperature and Salinity from the datasets examined in section *2*. As previewed, the connection between temperature and salinity is central to many ocean patterns, which is the subject of the final section of this paper (*5. AMOC and Thermohaline)*. Following the discussion of Equation [2] below, we'll return to the topic of salinity vs. temperature, as relevant for our purposes, in more equations.

Change in temperature in each of the 26 patches, or surface regions, is calculated on the basis of [1] and [2], and this is used to indirectly understand heat transport: cold water moves into patch *i*, thereby lowering temperature (*T*), but, at the same time, warming only affects this layer (the surface regions). This leads us to estimating *ocean heat uptake* in Equation [2].

OHU by Patch

Equation [2] is an integral used to calculate cumulative heat uptake through a patch *r* from 1871 to time *t*. Notice that the surface integral present in [1] is absent in [2]. This is reflected in the input variables on the left-hand side and their interpretation: we're no longer looking at the entire ocean as a whole surface; we're only interested in heat transport in a particular patch at one time. The 'scope' of [2] is of much narrower focus than [1], in a way, for measuring change in temperature. You need both equations, as mentioned, in order to understand heat transport in complex ocean processes: the big picture is given by [1] (prediction of OHC in the ocean's interior over V_R) while the details are given by [2] (OHU in a particular patch at each time). We'll complicate the picture even further (*4. Stewart & Hogg*) about how exactly is best to measure heat uptake, but so far we've improved from the simple ocean model in section *1*.

What do these PDEs tell us? Recall that OHC is a product of density (ρ), specific heat capacity (c_p), volume (V), and change in temperature (ΔT). While [1] and [2] above look quite complicated, the basic idea is clear:

$$\Delta V = A_i * \Delta SSH ,$$ where A_i = surface area of discretized surface patch;

SSH = sea surface height

$$\Delta SSH = \frac{\alpha\,(OHC)}{\rho * c_\rho} ,$$ where α = **thermal expansion coefficient**

To know something about OHC is to know something about change in volume and change in sea surface height of the ocean because water expands as it warms. The two equations above indicate the relationship between V and SSH (and OHC), and this brings us back to the topic of salinity and temperature, and the datasets we examined, as they are used in [1] and [2].

Salinity & Temperature Revisited

At last, we return to the topic of salinity vs. temperature and discuss its significance within the aims of our project. α, the **thermal expansion coefficient**, is calculated using Temperature and Salinity from the datasets we examined, as mentioned briefly earlier. (Crucially, this is *not* albedo, although they use the same letter, which may cause confusion.) α appears in the equation for change in sea surface height because the ocean expands when warmed, thus SSH measures the change in “level” (or flat) ocean waters with warmed (thus expanded) waters. This change impacts ocean volume, shown in the equations above. The equation for α is below:

$$\alpha = \quad -\frac{1}{\rho}\,\frac{d\rho}{dT} \qquad [3]$$

In other words, α is a function of -1/density multiplied by the derivation of density over temperature. What does this mean? [3] says that thermal expansion is inversely proportional to density. This makes intuitive sense: We know that water is denser when it is saltier, and when water is denser, and saltier, it is harder to warm; therefore, dense, salty water is colder as well. This is the central connection between the datasets we examined in section *2* and the GF reconstruction of OHC over time as studied by Zanna et al. (2019).

As we'll discuss in our final section (*5. AMOC and Thermohaline*), critical ocean processes are driven by the relationship between salinity and temperature as well. Salty, dense water form "deep water" currents that circulate throughout the world's ocean basins, thereby regulating ocean warming, by means of wind forcing (which warms the surface of the ocean), upwelling/downwelling, and the mixing of surface/warm and deep/cold ocean layers.

However, if salinity and temperature are so tightly intertwined, as we claim, then why did our findings in section *2* suggest that salinity does not play a large role in latent heat flux?

We know that latent heat flux is primarily driven by evaporation patterns, and our models supported the conclusion that latent heat flux is primarily influenced by temperature and regional climate dynamics, consistent with findings from Zanna et al (2019). They concluded that the majority of passive heat uptake in the ocean's interior is not through pathways at high latitudes but through midlatitude dynamics and thermodynamics; in particular, that substantial amounts of heat accumulated in the ocean (OHC/OHU) and associated sea level rise (SSH) can be influenced by low to midlatitude wind and air-sea fluxes and interactions (Zanna et al. 2019). If salinity matters for the thermal expansion coefficient (α) and the density of *(r,t)* in [1] and [2], what are we missing here?

This can be explained by complicating our understanding of ocean dynamics, particularly of the physical processes that occur at the ocean's surface. "Air-sea fluxes" may include evaporation, but a large factor that has not been discussed yet in detail is the influence of wind currents. At the ocean's surface, wind currents exert wind stress – a "drag force", i.e. a frictional force – on the surface of the ocean due to the friction between air and water. Wind stress drives vertical velocities through the wind stress curl – a "shear stress", i.e. a force parallel to a surface – which causes water to move and drives ocean currents. These dynamical forces at the ocean's surface influence warming and heat uptake. These factors bear heavily on latent heat flux, unlike sea surface salinity (SSS), which only plays a secondary role as our findings support.

So far, we've seen our findings are grounded in physical interactions that occur between the ocean and the atmosphere, which are also factors that further complicate ocean modelling. This concludes a brief introduction to wind-sea interactions as well as to the relationship between salinity, temperature, density, OHC, and dynamical forces. Further discussion continues in the following section on the challenges of complex ocean models, i.e. trying to take all of these factors into account.

4. ***Stewart & Hogg: A Complex Model (Angela)***

As we've seen, the ocean is extremely difficult to investigate and model. So far, we've moved from ODEs for a simple ocean model (imagined as an inert fluid) to PDEs for a slightly more complex ocean model (accounting for circulation indirectly by measuring and iterating change in temperature through surface regions). However, this improvement in methodology and representation does not capture all of the relevant information. It turns out that the *resolution* of one's model, particularly *vertical* resolution, significantly impacts predictions of heat and momentum uptake (Stewart & Hogg 2019). This is precisely because vertical resolution at the ocean's surface can make more precise predictions about the dynamical forces and physical processes of wind-sea interactions that were just described. In this section, we discuss these findings and consequences for future ocean modelling efforts.

As we saw, appealing to salinity, despite its close connection with temperature, was insufficient to explain latent heat flux patterns when examining the datasets in section *2*. This is why model resolution is important: representation of surface dynamics in ocean models governs the ability of the model to uptake heat (Stewart & Hogg 2019). Thus, their findings contribute to future comparisons of ocean models and present interpretations of existing models.

Surface Dynamics

Stewart & Hogg (2019) find that heat uptake depends only marginally on horizontal resolution, but instead depends heavily on vertical resolution at the ocean's surface. They explain attribute this result to the following reasons:

1. Surface vertical resolution influences ocean surface speed
2. Ocean surface speed influences wind stress exerted onto the model
3. Wind stress and curl are important factors for heat uptake

Thus, they predict that Southern Ocean heat uptake is sensitive to vertical resolution at the ocean's surface, which is a prediction that is borne out. They found that simulations with coarse surface vertical resolution exhibited heat content changes at rates nearly double that of simulations with finer vertical resolution. For ease of exposition, we'll use the names of the grids: ***GDFL50*** (10m) and ***KDS75*** (1.1m). All simulations demonstrated that the location of zero wind stress curl determined the location of maximum heat uptake. What do these findings mean?

In this section, we explain their findings in greater detail by appealing to the physical dynamics occurring at the ocean's surface introduced in the last section. Clarifying the impact of wind-sea interactions sheds light on the absorption and transport of heat between ocean basins (as in OHC/OHU from *sections 1 & 3*) and between the ocean and atmosphere (as in latent heat flux from *section 2*). Our explanations proceed by each numbered statement above.

First, why does surface vertical resolution influence ocean speed? According to Stewart & Hogg (2019), this is due to the momentum transfer between atmosphere and ocean: given the same wind field, the decreased ocean mass represented by thinner surface cells (e.g., ***KDS75***) are able to accelerate and respond to the wind variability more readily than thicker surface cells (e.g., ***GDFL50***). Ocean models typically use ocean surface speed to dynamically calculate the sensible heat and latent heat (evaporative) fluxes as well as wind stresses exerted onto the surface (by means of relative difference between wind and ocean surface velocities). Intuitively, a finer resolution grid is able to more efficiently model cause-and-effect relations from wind to ocean currents, thereby representing the influence of wind current velocity on ocean current velocity *faster*. In this way, the "cell" of the grid is "sensitive" to vertical resolution. Then, since wind stress depends on ocean surface speed, and ocean surface speed is sensitive to vertical resolution, we would expect the wind stress to be influenced by vertical surface resolution as well.

Second, why does wind stress depend on ocean surface speed? Recall that wind stress is a "shear stress," meaning that the force is exerted parallel to the surface it applies to. Wind stress is *parallel* to the ocean's surface due to the *Coriolis effect* deflecting wind currents. Recall that wind stress is also a "drag force," meaning that the force is a result of friction between two bodies – in this case, air and water. A stronger "drag force" is produced by greater friction between two bodies, but increased ocean surface speed is closer to the speed of the imposed wind perturbation in these simulations; thus, simulations with thinner surface cells (i.e., the finer vertical resolution) experience reduced wind stress because the ocean current velocity and wind current velocity have a smaller difference on account of the increased ocean surface speed. Then, since wind stress derives vertical velocities through the wind stress curl (N/m^3), which is the rate of change of direction of wind stress over a distance.

Third, why is wind stress curl an important factor for heat uptake? Recall that one finding was that "all simulations demonstrated that the location of zero wind stress curl determined the location of maximum heat uptake" (Stewart & Hogg 2019). What could explain this? For this, we'll introduce equation [4] for *Ekman pumping* (rate), given below:

$$w_{Ek} = \frac{\nabla \times \tau}{\rho_0 f} \qquad [4]$$

Ekman pumping is the vertical velocity at the base of the Ekman layer, i.e., the depth to which wind-driven transport extends which is about 100-150m. (Sometimes, Ekman pumping is used only to refer to downward (negative) velocity at the base of the Ekman layer, and *Ekman suction* is used to refer to the positive velocity.) In [4], the left hand-side w_{Ek} refers to *Ekman pumping*, while the right hand-side contains: ∇, a curl operator; τ, shear stress; ρ, density; *f*, Coriolis parameter. The numerator of the right hand side expresses the curl over the shear stress field ($\nabla \times \tau$), while the denominator expresses the density of seawater at a particular latitude (ρ * *f*). In the Southern Hemisphere, negative wind stress curl is upwelled (positive w_{Ek}) while positive wind stress curl is downwelled (negative w_{Ek}). This means that negative wind stress curl causes deep layers of water to rise; positive wind stress curl causes surface layers of water to sink.

Put another way, stronger winds (holding fixed ocean velocity, so we mean a greater difference in wind and ocean current velocities) can influence heat uptake by increasing the surface drag coefficient, which means that more energy is transferred from the ocean to the atmosphere. An increase in heat transfer to the atmosphere translates to a decrease in OHC. When water layers are mixed, the colder, deeper layers move up, and warmer, more buoyant layers move down, which overall reduces OHC as well.

We said earlier that one finding of Stewart & Hogg (2019) is that "All simulations demonstrated that the location of zero wind stress curl determined the location of maximum heat uptake." Now we can say why: zero wind stress curl means that there is no drag force or shear stress exerted on the ocean's surface, thus no heat is transferred from the ocean to the atmosphere in the production and expenditure of energy required for friction. So all heat absorbed into the ocean at these regions remains contained in the interior of the body of water, resulting in "maximum heat uptake." This concludes the discussion of wind forcing and patterns of wind-sea interactions that are sensitive to surface vertical resolution of a model. We hope that the discussion of the complex surface dynamics modelled by ocean simulations demonstrates some of the challenges of creating good ocean models for research purposes.

Consequences

Stewart & Hogg (2019) focus on the Southern Ocean (whereas the Zanna et al. (2019) focused primarily on the Atlantic Ocean). For their purposes, the Southern Ocean is a good candidate of study for two reasons: (1) Surface dynamics play an important role in Southern Ocean heat uptake; (2) Southern Ocean heat uptake plays an important role in predictions of the ocean's response to Earth's changing climate. For background, we note the following: (1) Southern Ocean is particularly sensitive to model biases in parameterization of air-sea fluxes and unresolved dynamics; (2) Southern Ocean warming accounts for 67-98% of total ocean warming since 2005 (Stewart & Hogg 2019). The pattern of warming in the Southern Ocean is complex, time-dependent, and inhomogenous. Heat uptake in this region is a result of surface fluxes of heat and momentum, ocean circulation, and the associated redistribution of existing oceanic heat reservoirs. Thus, investigation of Southern Ocean heat uptake requires detailed knowledge of these contributors, which all have non-trivial dynamics or representations (as we saw above) in climate and ocean models.

A consequence of these findings that Southern Ocean dynamics are sensitive to vertical resolution at the ocean's surface for ocean modelling is that efforts to increase horizontal resolution, such as in **CMIP6**, can be undermined if unaccompanied by adequate improvements to the vertical resolution (Stewart & Hogg 2019). We take this point to support our overall picture of the difficulties of ocean modelling due to subtle, interactive surface dynamics and the complex intrinsic patterns of the ocean's interior.

Equations [1] and [2] from section *3* showed some of the ways researchers attempt to investigate the ocean's interior (*indirectly*) in order to gain insight into OHC patterns over time (by comparison and inference). Equation [3] in section *3* was supposed to illuminate the density of *(r,t)* in [1] and [2] as well as shed light on our data analysis and conclusions in section *2*. Equation [4] in section *4* exemplifies some of the complex physical processes involved in seemingly simple ocean current patterns, and now we've seen evidence that even a difference of 9m in vertical grid resolution can significantly impact the predictions of the model. Despite all of these difficulties, as we attempted through our own analysis and modelling in section *2*, we still want to know what factors of the ocean contribute to its role in climate-regulation (SSS? SST?) as well as the exact nature of that regulation (warming patterns over time? OHC in 1871 vs today? Heat uptake as dependent on physical processes?). This is because of the singular and irreplaceable function of ocean circulation in keeping the planet cool.

5. ***AMOC & Thermohaline (Angela)***

We mentioned that heat uptake in the Southern Ocean plays a particularly important role in predictions of the ocean's response to Earth's changing climate. One special feature of the Southern Ocean basin is that it is the only ocean basin that touches every other ocean. The other ocean basins are separated by landmasses or do not directly "talk" to all the other ones. But this is not the case for the Southern Ocean: currents that flow outward from this region reach every other part of the world, mixing and rising and sinking (as a result of the physical forces previously discussed), before returning to their origisn. But the Southern Ocean is not the only ocean with an important role to play.

Thermohaline Circulation

To summarize, "Thermohaline Circulation" refers to when cold, dense water sinks in the polar regions, chiefly in northern North Atlantic (NADW) and around Antarctica (AABW), and then spreads into the rest of the ocean, gradually upwelling to feed a slow return flow to the sinking regions (AMOC, SOMOC). Any "out-flow" of deep water (cold, salty) into other oceans has to be balanced by "inflow" of upper-layer water (warm, bouyant) to replenish the fluid leaving because these are all closed systems. These processes drive circulation and allow deep water to travel everywhere, which is a major factor in climate regulation. As mentioned earlier, oceans "talk" to each other; in fact, circulation in the Southern Ocean is "to a large extent ... responsible for the anomalous cold, low-salinity state of the modern oceans" (Talley 2013).

AMOC & SOMOC

We can think of the global overturning circulation (GOC) as two connected overturning cells (Talley 2013). The GOC transports CO_2 and heat among the ocean basins and between the oceans and atmosphere. The "upper cell" comprises two parts: (1) North Atlantic Deep Water (NADW), and (2) Atlantic Meridional Overturning Circulation (AMOC). The "lower cell" comprises two parts as well: (1) Antarctic Bottom Water (AABW), and (2) Southern Ocean Meridional Overturning Circulation (SOMOC). AMOC is formed by the return flow of NADW, and has a depth range of 1500-3500m; SOMOC is formed by the return flow of AABW, and is "the deepest part of the abyssal ocean," i.e., the heaviest, saltiest, and coldest layer. These two cells in Talley's sense are interconnected via *upwelling* in the Southern Ocean, where deep waters are mixed in the circumpolar circulation. (Recall that, in general, these so-called “layers” intermix and exchange water, so it’s a kind of continuous system, not clear-cut categories.)

But what is “deep water” or “bottom water”? A body of water with a narrow range of temperature and salinity is called a “water mass,” and has a particular density. (Recall the 26 patches, defined based on density in a basin, of Zanna et al. (2019)’s methodology for GF reconstruction, and Equation [3].) “North Atlantic Deep Water” (NADW): There are three types of water masses that contribute to NADW. These are distinguished because they form in different areas but they share some common attributes: relatively warm (greater than 2 degrees C), and salty (greater than 34.9 parts per thousand). “Atlantic Bottom Water” (AABW): This type of water forms as a result of brine rejection, which is when the water around sea ice becomes saltier/heavier as a result of sea ice formation. Ice is just pure H_2O, so, to go from seawater to ice, the salt (brine) is “rejected” into the water around it. This heavier, saltier water has the following properties: salinity is 34.62 parts per thousand, temperature is -1.9 degrees C, and resultant density is 1.02789 grams per cm^3. Due to its high density after formation, AABW sinks and flows northward along the bottom – hence its name – into southern ocean basins around the world. These two types of water are the driving forces behind AMOC and SOMOC, creating the “Thermohaline Circulation.”

Stability of AMOC(Amy)

AMOC's stability has been a subject of significant research, with the possibility of it switching suddenly to another state having profound impacts on regional and global climates. The AMOC exhibits multiple equilibrium states, including a strong (warm) state and a weak (cold) state, and abrupt transitions between these states could happen. Such transitions are influenced by factors like freshwater input and temperature-salinity gradients. Recent studies have revealed that additional freshwater from the melting of the ice in Greenland and enhanced precipitation are reducing North Atlantic salinity, thereby destabilizing the AMOC and pushing it towards a tipping point (Ditlevsen & Ditlevsen, 2023). Paleoclimate records provide evidence of past abrupt AMOC changes linked to freshwater inputs, indicating the nonlinear behavior of the system (Rahmstorf, 2023).

Weakening of the AMOC would result in reduced northward heat transport, resulting in Europe's cooling and altered precipitation patterns vital for agriculture in regions like India, West Africa, and South America. Coastal areas, particularly on the eastern seaboard of the United States, might experience enhanced sea-level rise as a consequence of diminished ocean countercurrents, while tropical regions could see intensified warming. These changes can have cascading effects on ecosystems, like the potential dieback of the Amazon rainforest and increased instability of the Antarctic ice sheet.

Freshwater influx from melting ice sheets and glacial runoff is a factor destabilizing the AMOC. Climate models project a 34–45% decline in AMOC strength by 2100 under high-emission scenarios, with some suggesting a possible collapse from now to 2095 (Ditlevsen & Ditlevsen, 2023). Once collapsed, the AMOC's recovery could take centuries due to hysteresis effects, underscoring the urgency of implementing mitigation strategies .

Whereas CMIP6 models agree on the weakening trend of AMOC, they disagree on the timing and probability of a full collapse. Statistical approaches based on sea surface temperature proxies indicate earlier tipping points compared to process-based models, pointing out current observational gaps (Ditlevsen & Ditlevsen, 2023). Additionally, factors like Southern Ocean upwelling and wind-driven circulation might buffer against a full collapse, though this remains a topic of ongoing research.

The IPCC points out that rapid reductions in greenhouse gas emissions can prevent or postpone an AMOC collapse. However, current policies may not sufficiently address the nonlinear risks associated with AMOC instability, necessitating adaptive measures to ensure food security, infrastructure resilience, and disaster preparedness.

Relation with Heat Distribution(Amy)

The instability of the AMOC and the close coupling between ocean heat redistribution infers the ocean's dual capability as both a climate modulator and a heat sink. Referring to Zanna and her colleagues' work in the past, they proved that warming of the Atlantic Ocean was not only attributed to heat uptake at the surface but also heavily affected by heat convergence due to circulation. By using Green's functions to model heat transport pathways, they were able to calculate that around 50% of midlatitude Atlantic warming stemmed from changes in ocean currents, particularly reductions in northward heat transfer linked to a weakening AMOC (Zanna et al. 2019). This slowdown redirected heat to subtropical and midlatitude regions, hence undergoing a faster thermosteric sea-level increase (e.g., ~1 cm on the U.S. East Coast) as the warmer waters spread out (Zanna et al. 2019).

The AMOC's instability adds critical context to these findings. Paleoclimate records and modeling studies reveal that the AMOC has historically exhibited tipping-point behavior, where freshwater influx from ice melt or precipitation can trigger self-reinforcing feedbacks. For instance, reduced salinity in the North Atlantic decreases water density, weakening deep-water formation and further slowing the AMOC—a process termed the salt transport feedback (Rahmstorf 2024). This is consistent with Zanna et al.'s inference of heat accumulation driven by circulation because a weaker AMOC would decrease the northward transport of warm surface waters, with excess heat piling up in the mid-Atlantic (Zanna et al 2019.; Rahmstorf 2024).

Current climate models find it difficult to capture such dynamics. While Zanna et al. revealed the role of AMOC variability in redistributing heat, Rahmstorf notes that many models underestimate AMOC's bistability—its capacity to exist in "on" or "off" states, due to oversimplified representations of freshwater forcing and convection processes (Rahmstorf). Besides, low-resolution coarse vertical models can overestimate Ekman pumping and surface wind stress and over-bias deep-ocean heat uptake and AMOC sensitivity.

The biases highlighted the necessity to improve models for simulating AMOC's nonlinear responses more accurately, which are essential for regional climate impacts projections, for example, European cooling or tropical sea-level rise (Rahmstorf 2024; Banks & Gregory 2006).

Tipping Point & Oscillations(Amy)

The concept of a tipping point in the Earth's climate system refers to a crucial threshold that, when reached, a small perturbation can trigger a component into a qualitatively new state from which it may be virtually impossible or very hard to return to the original state (Lenton et al. 2008). In simplified box‑model frameworks, this behavior emerges from a saddle‑node bifurcation: a feedback loop in which reduced northward heat transport cools surface waters in the North Atlantic, thereby enhancing buoyancy anomalies and suddenly inactivating deep convection after a set threshold of freshwater has been achieved (Lenton et al. 2008).

Numerical models in large-scale coupled general-circulation models verify this threshold response, demonstrating that sustained freshwater inputs, either from increased ice-sheet melting or anomalously vigorous precipitation, have the ability to destabilize the AMOC. When freshwater forcing exceeds a few tenths of a Sverdrup, these models typically demonstrate an abrupt, rather than gradual, weakening of the overturning circulation. As a result of nonlinear hysteresis, restoring the original circulation requires removal of freshwater well beyond the initial perturbation, emphasizing the irreversibility associated with crossing the tipping point. In addition, other feedbacks, such as sea‑ice albedo, and wind‑driven Ekman transport, modify the precise threshold and recovery path but preserve the intrinsic nonlinear character of the transition (Lenton et al. 2008).

Composed with this potential for abrupt shift is the AMOC's intrinsic multidecadal variability. Chen and Tung (2018) demonstrate that, contrary to expectations from preindustrial‑condition models, the observed minimum of the AMOC between 1975 and 1998 occurred during a time of rapid surface warming, rather than cooling (Chen and Tung 2018). In conditions of strong greenhouse‑gas forcing, the AMOC's dominant function changes from poleward heat transport—region-wide warming of the North Atlantic—to acting as a planetary heat sink, sequestering excess heat at depth. During the mid‑1990s speeding phase, the AMOC held about half of the remaining global heat uptake, driving the so‑called "global‑warming hiatus," while its subsequent weakening has been blamed largely for internal variability rather than a monotonic forced trend (Chen and Tung 2018).

In order to predict future AMOC behavior, it is therefore important to distinguish intrinsic oscillations from the trend towards an actual tipping point. Natural variability may hide or postpone early warning signals, such as increasing autocorrelation and variance in key observational indices, hence making it problematic to assess proximity to threatening thresholds (Lenton et al. 2008; Chen and Tung 2018). People continue to do early refinement of observational and modelling, warning systems are therefore important in order to assess vulnerability of the AMOC to sustained anthropogenic freshwater forcing and to predict the likely chance for abrupt climate transitions.

6. ***Conclusion (Angela)***

In this paper, we presented our own findings from modelling data obtained from two ECCO-GODAE datasets – the first for sea surface salinity (SSS), and the second for sea surface temperature (SST) values – and one NCEI dataset, for latent heat flux (LHTFL) data. Our findings align with conclusions by Zanna et al. (2019), and we explained these conclusions by appealing to dynamical processes that occur at the ocean's surface. Various factors – properties of water (*section 1*); evaporation and regional climate dynamics (*section 2*); salinity, temperature, and wind (*sections 3 & 4*) – contribute to the difficulties of ocean modelling. The complexities of these processes are corroborated by findings from Stewart & Hogg (2019) about the sensitivity of model simulations to vertical resolution. Finally, we concluded with the importance of oceans in climate-regulation by means of global circulation patterns that distribute heat (*section 5*), thereby keeping our lovely little planet livable for just a bit longer.

Citations

Banks, Helene T., and Jonathan M. Gregory. "Mechanisms of Ocean Heat Uptake in a Coupled Climate Model and the Implications for Tracer Based Predictions of Ocean Heat Uptake." Geophysical Research Letters, vol. 33, no. 7, 2006, https://doi.org/10.1029/2005gl025352.

Boyer, Tim. "Global Ocean Heat and Salt Content - Heat Content Monthly Global Analyzed Fields." *National Centers for Environmental Information (NCEI)*, www.ncei.noaa.gov/access/global-ocean-heat-content/heat_global.html. Accessed 29 Mar. 2025.

Centre, AHA, and About AHA Centre. "Vol 66 – Getting to Know El Niño & La Niña - AHA Centre - The Column." *AHA Centre - The Column - The AHA Centre News Bulletin*, 30 Nov. 2020, thecolumn.ahacentre.org/insight/vol-66-getting-to-knnina/.

Chen, Xianyao, and Ka-Kit Tung. "Global Surface Warming Enhanced by Weak Atlantic Overturning Circulation." Nature, vol. 559, no. 7714, July 2018, pp. 387–391, www.nature.com/articles/s41586-018-0320-y, https://doi.org/10.1038/s41586-018-0320-y.

Chase Academy. "Thermohaline Circulation; Deep Water Currents & Water Mass." *Chase Academy*, 8 Aug. 2024, chaseacademy.in/thermohaline-circulation-deep-water-currents-water-mass/.

Ditlevsen, Peter D., and Susanne Ditlevsen. "Warning of a Forthcoming Collapse of the Atlantic Meridional Overturning Circulation." Nature Communications, vol. 14, no. 1, 2023, article no. 4254. https://doi.org/10.1038/s41467-023-39810-w.

Earth 103: Earth in the Future. "Albedo." www.e-education.psu.edu/earth103.

"Estimating the Circulation and Climate of the Ocean (Ecco)." *NASA*, NASA, 21 Sept. 2023, podaac.jpl.nasa.gov/ECCO?tab=mission-objectives&sections=about%2Bdata.

Pontes, Gabriel M, and Laurie Menviel. "Weakening of the Atlantic Meridional Overturning Circulation Driven by Subarctic Freshening since the Mid-Twentieth Century." Nature Geoscience, 18 Nov. 2024, www.nature.com/articles/s41561-024-01568-1, https://doi.org/10.1038/s41561-024-01568-1.

Hautala, Susan. "Ekman Pumping." *Physics Across Oceanography Fluid Mechanics and Waves*, University of Washington, 15 Dec. 2020, uw.pressbooks.pub/ocean285/chapter/ekman-pumping/.

Hautala, Susan. "The Curl, and Vorticity." *Physics Across Oceanography Fluid Mechanics and Waves*, University of Washington, 15 Dec. 2020, uw.pressbooks.pub/ocean285/chapter/ekman-pumping/.

"How Seawater Moves: Ekman Transport ." *UCAR Center for Science Education*, NESTA, 2008, scied.ucar.edu/learning-zone/earth-system/how-ocean-moves-ekman-transport.

Lenton, T. M., et al. "Tipping Elements in the Earth's Climate System." Proceedings of the National Academy of Sciences, vol. 105, no. 6, 7 Feb. 2008, pp. 1786–1793, www.pnas.org/doi/full/10.1073/pnas.0705414105, https://doi.org/10.1073/pnas.0705414105.

Libretexts. "2.14: Water - High Heat Capacity." Biology LibreTexts, 23 Nov. 2024, bio.libretexts.org/Bookshelves/Introductory_and_General_Biology/General_Biology_(Boundless)/02%3A_The_Chemical_Foundation_of_Life/2.14%3A_Water_-_High_Heat_Capacity.

Rahmstorf, Stefan. "Is the Atlantic Overturning Circulation Approaching a Tipping Point?" Oceanography, vol. 37, no. 3, 1 Jan. 2024, https://doi.org/10.5670/oceanog.2024.501

Stewart, K. D., & A.McC. Hogg. "Southern Ocean heat and momentum uptake are sensitive to the vertical resolution at the ocean surface." *Ocean Modelling*, vol. 143, Nov. 2019, https://doi.org/10.1016/j.ocemod.2019.101456.

US Department of Commerce, National Oceanic and Atmospheric Administration. "The Ekman Spiral." *Currents: NOAA's National Ocean Service Education*, National Ocean Service: National Oceanic and Atmospheric Administration, 1 June 2013, oceanservice.noaa.gov/education/tutorial_currents/04currents4.html.

Vallis, Geoffrey K. "THE OCEAN'S OVERALL ROLE IN CLIMATE." Climate and the Oceans, vol. 5, Princeton University Press, 2012, pp. 105–27. JSTOR, https://doi.org/10.2307/j.ctt7s6vr.8. Accessed 10 May 2025.

Zanna, Laure, et al. "Global reconstruction of Historical Ocean Heat Storage and Transport." *Proceedings of the National Academy of Sciences*, vol. 116, no. 4, 7 Jan. 2019, pp. 1126–1131, https://doi.org/10.1073/pnas.1808838115.